On-orbit Radiometric Calibration Over Time and Between Spacecraft Using the Moon

Hugh H. Kieffer[a], Thomas C. Stone[a], Robert A. Barnes[b], Steven Bender[c], Robert E. Eplee Jr.[b], Jeff Mendenhall[d], and Lawrence Ong[e]

[a] U.S. Geological Survey, 2255 N. Gemini Drive, Flagstaff AZ, 86001
[b] SeaWiFS Project, Code 970.2, NASA/Goddard Space Flight Center, Greenbelt, MD 20771
[c] Los Alamos National Laboratory
[d] Lincoln Labs, MIT
[e] EO-1 Project - SSAI, Code 923, NASA-Goddard Space Flight Center, Greenbelt, MD 20771

ABSTRACT

The Robotic Lunar Observatory (ROLO) project has developed a spectral irradiance model of the Moon that accounts for variations with lunar phase through the bright half of a month, lunar librations, and the location of an Earth-orbiting spacecraft. The methodology of comparing spacecraft observations of the Moon with this model has been developed to a set of standardized procedures so that comparisons can be readily made. In the cases where observations extend over several years (e.g., SeaWiFS), instrument response degradation has been determined with precision of about 0.1% per year. Because of the strong dependence of lunar irradiance on geometric angles, observations by two spacecraft cannot be directly compared unless acquired at the same time and location. Rather, the lunar irradiance based on each spacecraft instrument calibration can be compared with the lunar irradiance model. Even single observations by an instrument allow inter-comparison of its radiometric scale with other instruments participating in the lunar calibration program. Observations by SeaWiFS, ALI, Hyperion and MTI are compared here.

Keywords: Moon, on-orbit calibration, spacecraft

1. INTRODUCTION

The advantages and complications of using the Moon as a calibration target for Earth-orbiting spacecraft have been previously discussed.[1–6] The intrinsic stability of the lunar surface photometric properties[7] means that a lunar radiometric model can be applied to observations made at any time. A corollary is that observations of the Moon made by the same or different spacecraft at diverse times can be inter-compared through use of a lunar radiometric model. This has the potential of interrelating the calibration scales of all spacecraft which view the Moon. Several orbiting instruments have made observations of the Moon specifically for calibration, and results from four of these are described here. The primary objective for each of these instruments has been to monitor response over time, which does not require an absolute scale for the lunar spectral model. However, comparisons between instruments require that the lunar model spectral irradiance is close to the correct scale and that the variations with wavelength are correct. The lunar model used here is tied to the star Vega for absolute scale and uses measurements of returned Apollo samples to remove residual spectral variations.

It must be emphasized that the absolute scale of the ROLO lunar irradiance model is somewhat uncertain.[8] At the level of precision being obtained and at the potential sub-percent level of accuracy, the radiometric scale of the Moon may ultimately depend either on new approaches with above-the-atmosphere direct traceability to international radiometric standards or adjudication between observations of the Moon by a large number of instruments with many different calibration pathways.

Further author information: (Send correspondence to H.H.K.)
E-mail: hkieffer@usgs.gov; telephone: 928-556-7015; fax: 928-556-7014
T.S.: e-mail: tstone@usgs.gov

Spacecraft normally view the Moon for calibration purposes with the phase angle (Sun-Moon-spacecraft angle) near ± 4 to 10° (phase angle is strictly a positive quantity, however it is convenient to use negative values to distinguish observations made before full Moon). These phase angles catch the Moon near its maximum brightness, but avoid both eclipse phenomena and the radiance uncertainties associated with the Moon's strong and narrow backscatter peak. The apparent diameter of the Moon (expressed in nominal nadir surface distance from a 705 km altitude orbit) ranges from 6.2 km (at apogee) to 6.8 km (perigee).

Complete lunar images can be compared directly with models of lunar irradiance to generate instrument gain factors. For high spatial resolution instruments, which may not quite capture the entire Moon, information on the absolute scan orientation can be used to correct reasonably well for the missing segment. Because the Moon is variegated, radiometric analysis of partial lunar images properly requires comparison to a spatially resolved lunar radiometric model, which is being developed from the ROLO observing program.[2,6] For now, a simple area factor is used; this implicitly assumes that the average brightness in the missing portion is the same as in the imaged portion.

2. THE ROLO LUNAR IRRADIANCE MODEL

The goal of the ROLO lunar irradiance model is to fit calibrated telescopic observations for each band used to the extent that there is no correlation within the residuals. The analytic form used for this fit has evolved as our modeling has improved. The version presented here, 311f, has a mean absolute residual of 0.96% across all ROLO bands.

The model operates in distance-corrected reflectance, wherein the calibrated radiance images are corrected to exoatmospheric radiance, integrated to irradiance, have both a solar and observer $1/R^2$ correction applied to reduce the observations to standard distances from the Moon to the Sun (one Astronomical Unit or 149.598 10^9 km) and to the observer (384,400 km), and are then converted to disk-equivalent reflectance by the relation:

$$I_k = A_k \cdot \Omega_M E_k / \pi \tag{1}$$

where A_k is the disk-equivalent albedo (reflectance), Ω_M is the solid angle of the Moon and E_k is the solar spectral irradiance at the effective wavelength λ_{Sk} of a band for solar radiation, the last two both at standard distance; Ω_M =6.4236×10^{-5} steradian. This conversion involves a solar spectral irradiance model, which may have significant uncertainties in some wavelength regions. However, the direct dependence on solar model cancels to first order as long as the same model is used in going from irradiance to reflectance and back.

All work thus far has ignored variation with time of the solar spectral irradiance; the variation of total solar irradiance is about 0.2 %[9] although variation in the ultraviolet is considerably greater.

To fit the ROLO observations, we have used an empirical analytic form based on the primary geometric variables:

$$\ln A_k = \sum_{i=0}^{3} a_{ik} g^i + \sum_{j=1}^{3} b_{jk} \Phi^{2j-1} + c_1\theta + c_2\phi + c_3\Phi\theta + c_4\Phi\phi + d_{1k}e^{-g/p_1} + d_{2k}e^{-g/p_2} + d_{3k}\cos((g-p_3)/p_4) \tag{2}$$

where g is the absolute phase angle, θ and ϕ are the selenographic latitude and longitude of the observer and Φ is the selenographic longitude of the Sun.

The first polynomial represents the basic photometric function dependence upon phase angle, disregarding any opposition effect. The second polynomial approximates the dependence upon the face of the Moon that is illuminated, primarily representing the distribution of mare and highlands. The four terms with coefficients c_n represent the face of the Moon that is seen (topocentric libration), with a consideration of how that is illuminated. The form of the last three terms, all non-linear in g, is strictly empirical: the first two represent the opposition effect and the last one is simply to address a correlation seen in the irradiance residuals.

Exclusion of outlier points leaves about 1200 observations for each filter. Eight values are treated as constant over wavelength; the 4 c terms for libration and the 4 g nonlinear parameters. There are 9 additional values for each filter, for a total of 296 coefficients. The mean absolute residual over the 36648 observations is 0.0096 in natural logarithm of irradiance. No significant relation has been found between these residuals and any of the geometric parameters, including selenographic latitude of the Sun.

Table 1: Lunar Irradiance Model Coefficents

Symbol	Term	Name	Value	Units	Effect
a_0	g^0	Constant	-1.889	–	
a_1	g^1	Phase 1	-1.627	radian^{-1}	2.811
a_2	g^2	Phase 2	0.438	radian^{-2}	1.309
a_3	g^3	Phase 3	-0.235	radian^{-3}	1.212
b_1	Φ^1	SunLon 1	0.0425	radian^{-1}	0.147
b_2	Φ^3	SunLon 3	0.0132	radian^{-3}	0.137
b_3	Φ^5	SunLon 5	-0.005	radian^{-5}	0.157
c_1	θ	Libr X	0.0003	deg^{-1}	0.005
c_2	ϕ	Libr Y	-0.0014	deg^{-1}	0.028
c_3	$\Phi\theta$	SunLon*LibX	0.0010	deg^{-1} radian^{-1}	0.026
c_4	$\Phi\phi$	SunLon*LibY	0.0006	deg^{-1} radian^{-1}	0.017
d_1	e^{-g/p_1}	1st expon.	0.389	–	0.264
d_2	e^{-g/p_2}	2nd expon.	-0.148	–	0.130
d_3	$\cos((g-p_3)/p_4)$	cosine	-0.0035	–	0.004
p_1		1st expon.	3.98	degree	
p_2		2nd expon.	12.19	degree	
p_3		phase	-43.48	degree	
p_4		period	18.73	degree	

2.1. Magnitude of lunar variation (libration and phase)

The values of each model coefficient or parameter, averaged over all ROLO bands, are given in Table 1. These values should not be used to compute lunar albedo at a particular wavelength, but are simply representative of the importance of each term. The "Effect" column indicates the magnitude of the change in $\ln A$ for each term over the full range of its variables. The total effect of libration is about 5%, of which the first two terms (without Φ) constitute about 2.5%; these magnitudes are similiar to estimates made by integrating the albedo of appropriate faces of the Moon using a digital map constructed from Clementine data.[10]

2.2. Adjusting the absolute scale versus wavelength

The solar irradiance in Eq. 1 is assumed constant for each band. It is derived from the model of Wehrli,[11] and is calculated using:

$$E_k = \frac{\int_{\lambda_1}^{\lambda_2} E(\lambda) R_k(\lambda) d\lambda}{\int_{\lambda_1}^{\lambda_2} R_k(\lambda) d\lambda} \tag{3}$$

where $E(\lambda)$ is the solar spectral irradiance at 1 A.U., $R_k(\lambda)$ is the band's system relative spectral response, and the limits for the integrals are the wavelengths over which the spectral response is measured.

The model derived by direct fit to the ROLO observations using a star-based nightly calibration yields reflectance spectra which have modest excursions in wavelength between bands, whereas the reflectance spectrum of the Moon has only weak, broad features.[12–15] The laboratory reflectance spectrum of returned Apollo soil samples[16] was used to adjust the scale of each wavelength*. The soil spectrum was scaled $A' = (a + b\lambda)A$ to fit the ROLO irradiance spectrum for $g = 7°$, $\Phi = 7°$, $\theta = 0$, $\phi = 0$. The adjustment factor for each ROLO filter is that required to match the ROLO model to the scaled Apollo spectrum; the average correction is 3.5%. The lunar highlands exhibit greater depth for the FeO bands near 950 nm and 1900 nm than do the mare,[14,15] so that the Apollo soil sample may under-estimate these band strengths for the Moon. Thus, the adjustment used here may over-estimate by a few percent the lunar radiance near 950 nm and 1900 nm.

*This spectrum is available at http://www.planetary.brown.edu/pds/AP62231.html

2.3. Comparison with Spacecraft

For comparison with spacecraft instrument bands, the ROLO model is interpolated in wavelength to the effective wavelength of the spacecraft instrument band for a nominal lunar spectrum. Because the Moon's reflectance spectral features are broad and shallow, wavelength interpolation of the lunar model is done in reflectance, using linear interpolation with an additional shape factor that preserves the detailed shape of the Apollo reference spectrum between the ROLO observation wavelengths.

The ROLO team has adopted a "percent disagreement" as the standard of comparison between spacecraft and ROLO irradiance results;

$$P = 100 \left(\frac{I_{\mathrm{SC}}}{I_{\mathrm{ROLO}}} - 1. \right) \tag{4}$$

3. GENERIC SPACECRAFT OBSERVATION OF THE MOON

Typially, lunar scans are accomplished by re-orienting the spacecraft from pointing toward the center of the Earth to pointing near the Moon; this maneuver begins roughly when the spacecraft enters the Earth's shadow. The instrument optical axis (spacecraft nadir boresight) should scan past the Moon in the "down-track" dimension so that a normal image is constructed; usually this image is elongated in the image Y axis direction. The entire attitude manuver may be single pitch, adding (or subtracting) one revolution to the normal nadir-locked rate, or a compound maneuver that points the spacecraft near the Moon then pitches past it at a uniform rate. Commonly, the spacecraft regains its normal orientation before leaving Earth's shadow.

The pitch passing over the Moon should be at a constant rate, as this corresponds to uniform sampling of the Moon. This pitch should extend at least a degree or so beyond the edge of the Moon to allow sampling of space beyond the extended point-spread-function in all bands. Commonly, the pitch rates are set so that the angular velocity of the Moon past the detector is 4 to 8 times slower than the angular velocity of a normal nadir scene, leading to an oversampling factor in the line direction of this factor.

In the simplest lunar calibration method, spacecraft observations of the Moon are reduced to irradiance, corrected for oversampling, and compared with the irradiance predicted for each band at the same illumination and observing geometry.

The generic steps for spacecraft team processing of a spacecraft lunar observation to produce a lunar irradiance measure are outlined in Ref. 17. In summary, these are:

- Determine the approximate location of the Moon in the image.
- Use the neighboring region of the image outside any scattered light flare to determine the dark level for each detector.
- Subtract the dark level[s] and calibrate the image to radiance.
- Determine the precise extent of the Moon in the spacecraft motion direction.
- Determine the (elliptical) region of the image which includes lunar radiation. If the lunar image is incomplete, determine the clip angle and missing radial extent.
- Sum the image over this region and multiply by the nominal solid angle of a pixel to produce apparent irradiance.

4. DIGITAL DATA EXCHANGE PROTOCOL

A lunar calibration involves exchanging information between the spacecraft instrument team (SCT) and the ROLO lunar calibration team (LCT). As the number of participating instruments has increased, it has been useful to adopt standard formats and proceedures for this exchange. For instruments with fewer than about 16 bands, two pure ASCII files are prepared by the spacecraft instrument team. Each file begins with a "keyword=value" label section that is followed by a tabular section containing a row for each lunar observation. The files have strict row correspondance in the tables; one contains columns for the time and spacecraft position for each lunar observation, and the other columns for the apparent irradiance for each band and the lunar image size. Currently there is no treatment for the small variation of geometry over the few seconds typically required to scan across the Moon. The SCT also processes the image to derive the apparent irradiance without

consideration of the oversampling factor, and determines the apparent angular size of the Moon in the spacecraft scan direction. For instruments with many bands (arbitrarily chosen as more than 16) the number of columns for a multi-observation file becomes impractical, so geometry and radiometry are combined into a single file for each observation.

Upon receipt of these files, the LCT uses the spacecraft observation time to compute the precise position of the Earth and Moon relative to the Sun and the orientation of the Moon in the J2000 coordinate system using the double-precision planetary ephemeris DE200. From these values, all relevant geometric angles and distances are computed. The true angular size of the Moon and the apparent angular size provided by the SCT are used to compute the oversample factor. The ROLO lunar irradiance model is interrogated at the appropriate geometric angles and scaled from standard distances to the Sun and spacecraft distances at the time of the observation. These values are interpolated in wavelength to the effective wavelengths of the spacecraft instrument bands. Finally, the difference percentage is computed. These results are written to a paired geometry and irradiance files that are striclty parallel to the SCT files, and returned to the SCT. Full specification and examples of all files are available at **www.moon-cal.org** → Spacecraft Calibration → Multiple Observation Files.

5. RESULTS FOR FOUR INDIVIDUAL INSTRUMENTS

5.1. Philosophy

Vicarious calibrations such as lunar views, can be used to determine the stability of an instrument or to determine the consistency of the standard products derived from its observations. There must be unambiguous understanding between the instrument team and the vicarious calibration team over which approach is being used. In the first case, the lunar images must be processed with a constant set of calibration coefficients, typically based upon pre-launch calibration. In the second case, the lunar images are processed with the same set of calibration coefficients as are used to produce standard products, and this set commonly depends upon the date of observation. The two sets of calibration coefficents may differ in complex ways, commonly based upon an improved understanding of the true nature of an instrument developed after launch. A state may be reached where it is no longer useful to use the prelaunch calibration; e.g., it is determined on-orbit that the instrument response depends upon parameters that were not measured before launch. For most instruments, a natural transition from the first to the second situation will occur, after which lunar calibration comparisons determine not the instrument history, but the residuals from the instrument teams' modeling of the instrument. It is in this latter environment that comparisons between instruments should occur; however, this level has been reached only for SeaWiFS thus far.

5.2. SeaWiFS

SeaWiFS is an eight band filter radiometer designed to monitor Earth-exiting radiances from ocean scenes.[18,19] The nominal center wavelengths for the SeaWiFS bands[20] are given in Table 2. The actual center wavelengths for measurements on orbit are within about 1 to 2 nm of these valuess. Also listed are the effective wavelengths for a nominal lunar spectrum, determined by detailed convolution of the SeaWiFS band relative spectral response, the solar spectrum, and the nominal spectral reflectivity of the Moon.

The sensor's instantaneous field of view is 1.6 mrad by 1.6 mrad per pixel, with one scan covering 58.3 deg on either side of nadir. From a measurement altitude of 705 km, this gives Earth measurements, at nadir, that are 1.1 km on a side. SeaWiFS can be biased +20°, 0°, or -20° from nadir in the direction of flight to minimize the effects of ocean glint on the data. Each measurement is digitized to 10 bits, with a typical signal level of 600 digital numbers (DN) and a noise of 1 DN or less. The results of the prelaunch characterization of SeaWiFS are summarized in Barnes et al. (1994).[20]

SeaWiFS operates in a Sun synchronous orbit, crossing the Equator from north to south at local noon. In normal operation the spacecraft is maintained in a nadir orientation, using pitch-axis momentum wheels for attitude control, with a spacecraft pitch rate of 360° per orbit (about 0.06° per second). For lunar measurements, the rotation rate of the momentum wheels is increased, and the spacecraft is pitched in the opposite direction at a rate faster than the Earth view (0.15° / second). The maneuver is started past the South Pole passage and is timed such that SeaWiFS will view the moon as the spacecraft ground track passes the sub-lunar point. At

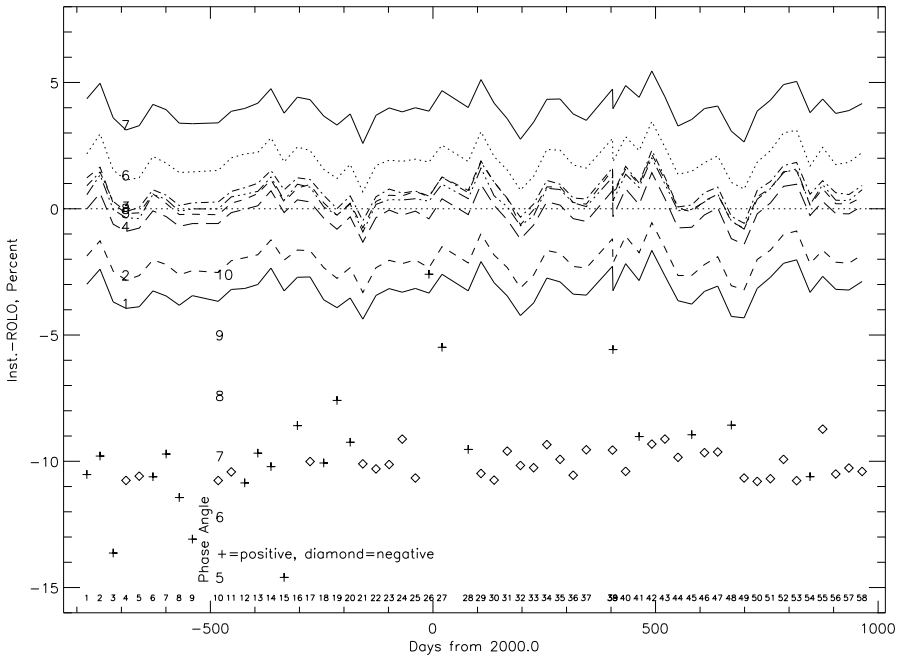

Figure 1. Absolute response of SeaWiFS bands versus time after asymptotic trend correction. Successive lunar observations are indicated along the bottom of the figure; numbers 38 and 39 were taken 1/2 day before and after Full Moon. Curves indicate SeaWiFS calibrated irradiance relative to ROLO lunar model, in percent; diamonds indicate phase angle before Full Moon; scale is indicated as numbers above the -500 day tick; plus signs are phase angle after Full Moon.

Table 2: SeaWiFS Band Wavelengths and Corrected Drift.

SeaWiFS Band	Nominal Wavelength (nm)	Effective Wavelength for Moon (nm)	Disagreement Initial % 0.13	Disagreement Drift %/year 0.05	<|resid|> <– Uncert.
1	412.	414.35	-3.39	0.09	0.45
2	443.	444.83	-2.23	0.07	0.45
3	490.	491.61	0.55	0.07	0.46
4	510.	510.03	-0.30	0.07	0.45
5	555.	554.93	0.26	0.07	0.47
6	670.	668.55	1.80	0.06	0.47
7	765.	766.07	3.81	0.06	0.46
8	865.	866.47	0.38	0.05	0.50

the end of the maneuver, about 28 minutes later, when the spacecraft again points toward Earth, the pitch rate is returned to normal. During views of the Moon, the scan direction of SeaWiFS is such that the instrument scans across the lunar surface from west to east in celestial coordinates.

SeaWiFS has been making observations of the Moon nearly every month since 1997 Nov, usually with phase angle near 7° either before or after Full Moon; descriptions of SeaWiFS lunar calibration are provided by Refs. 3, 4, 21. Some SeaWiFS bands have the unusual complication of noise levels so low that the dark level can only be determined to the nearest integral DN.[22] The SeaWiFS nominal resolution and a line oversampling factor for the Moon of about 4 result in a lunar image of about 6 samples by 24 lines; this is the smallest image which has been used for lunar calibation to date.

The absolute calibration results for the first 50 lunar observations indicated that the first six bands exhibit little change. Band 7 has shown about a 4% drop, and Band 8 about a 10% drop. Based upon lunar observations

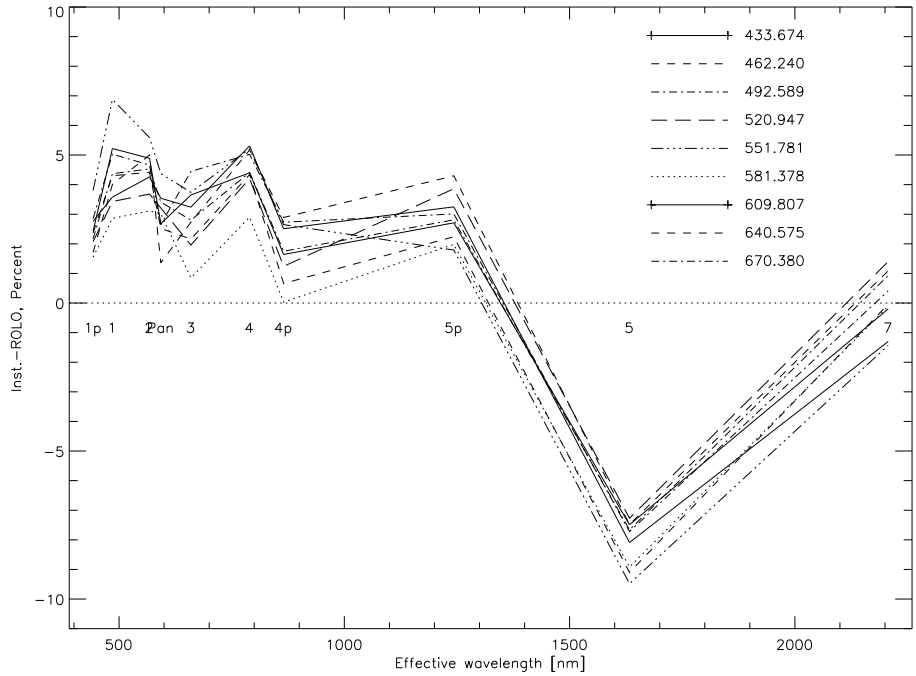

Figure 2. Percent disagreement spectra for EO-1 ALI; data are shown for 9 successive lunations. The patterns are consistent at the sub-percent level

the SeaWiFS team has developed an asymptotic time correction for SeaWiFS radiances[23] of the form:

$$L_i' = L_i \left[a_{i,0} - a_{i,1} \left(1. - e^{-a_{i,2} t} \right) \right]^{-1} \tag{5}$$

When this correction is applied, the lunar calibration observations have negligible trend, $< 0.1\%$ per year; see Fig. 1. The responsivity of each band was fit as a linear function of time; the results are listed in Table 2. Each observation was assigned a one-sigma uncertainty of 0.5%, the resulting formal uncertainty of the initial irradiance disagreement and of the remaining drift rates are listed at the tops of those columns. There is currently no explanation for the $\pm\frac{1}{2}\%$ coherent variation.

5.3. ALI

The Advanced Land Imager is a technology demonstration instrument built at MIT Lincoln Laboratory and serves as a test-bed to validate emerging technologies for future land-imaging instruments.[24] The ALI was launched on November 21, 2000 aboard the EO-1 spacecraft and is in an orbit one minute behind Landsat 7. The key technologies being tested on the ALI include large, wide field-of-view silicon carbide optics, compact multi-spectral arrays, non-cryogenic (220 K) HgCdTe detectors, and a novel solar calibration technique. The telescope is an f/7.5 reflective triplet design with a 12.5-cm unobscured entrance pupil and a 15° cross-track by 1.25° in-track field-of-view. The optical design features a flat focal plane and telecentric performance, which greatly simplifies the placement of the filter and detector array assemblies.

Although the optical system supports a 15° wide field-of-view, only 3° (37 km cross-track) was populated with detector arrays for the technology demonstration. If the focal plane were fully populated, the detector arrays would cover a 185-km swath on the ground, equivalent to Landsat, in a 'push-broom' mode. The multi-spectral panchromatic (MS/Pan) array has 10 spectral bands in the visible, near infrared (VNIR) and short wave infrared (SWIR) (Table 3). Six of the nine multi-spectral bands are the same as those of the Enhanced Thematic Mapper (ETM+) on Landsat 7 for direct comparison of data. The Panchromatic band has 10-m Ground Sample Distance (GSD), all the other bands have 30-m GSD.

Table 3: ALI Band Wavelengths and Irradiance Comparison.

ALI Band	Nominal Wavelength (nm)	Wavelength Range for Moon (nm)	Effective Wavelength % 0.31	Disagreement Initial %/year 0.80	Disagreement Drift <– Uncert.	<|resid|>
1p	442.	433-453	442.39	2.53	-0.35	0.47
1	485.	450-515	485.35	4.15	0.79	0.87
2	567.	525-605	567.60	4.51	-0.16	0.53
Pan	592.	480-690	592.72	2.78	0.59	0.60
3	660.	630-690	659.54	3.25	-1.27	0.82
4	790.	775-805	789.76	5.12	-1.77	0.45
4p	865.	845-890	865.28	2.66	-2.69	0.65
5p	1245.	1200-1300	1242.94	3.58	-2.15	0.55
5	1640.	1550-1750	1632.93	-7.84	-0.90	0.68
7	2225.	2080-2350	2207.11	-0.10	0.56	0.80

Lunar observations using the ALI have been conducted near a 7° phase angle each month since January 2001. For each observation, the spacecraft is maneuvered to scan the Moon in the in-track direction at 1/8 the nominal scan rate in order to oversample the disk. A region of interest, narrowly circumscribing the Moon, is then defined by locating the region of each column where the intensity falls to below 1% of the average lunar irradiance. The lunar spectral irradiance is obtained by summing the calibrated image within the circumscribed region.

Once the measured lunar irradiance has been determined for a given observation, the expected lunar irradiance for the time of the observation is calculated using the ROLO lunar model. The lunar comparison disagreement spectra are shown in Fig. 2.

5.4. Hyperion

The EO-1 Hyperion spectrometer is the first imaging spectrometer in permanent Earth orbit. It has a nominal 30-m resolution in 242 bands covering 356 to 2577 nm, although 200 bands from 397 to 2406 nm have useful response. The Full Moon barely fits in the Hyperion swath, and EO-1 was pointed at the Moon for Hyperion on alternate months beginning in 2001 Feb, usually clipping the Moon at one edge. For the clipped images, a simple area-ratio correction has been applied. Early results were reported in Ref. 17. In 2001 Nov. and later, the image usually captured the entire Moon. Based on comparison with other spacecraft, the EO-1 project has adjusted the pre-launch calibration response below 840 nm down by 8% and the response above 940 down by 18%. Only a few lunar observations have been calibrated with the revised coefficients and processed to lunar irradiance; these are shown in Fig. 3. The abundant "jitter" in the disagreement spectra is similar to that derived from observations of a dry lake in Australia.[25]

5.5. MTI

The Multi-spectral Thermal Imager (MTI) is a DOE imager that has 10 bands in the solar reflection wavelength region, with a nominal GSD of 5 m in the VNIR and 20 m in the SWIR at a 575-km altitude. There are five longwave IR bands which also have 20-m GSD.

MTI has three identical focal-plane sensor chip assemblies (SCAs). Each SCA spans approximately 0.47° and the combined cross track extent is 1.38° due to overlap. The center SCA has a reverse band orientation in the along-track direction so that the four highest resolution bands are close to the instrument's optical axis. Imaging of the Moon typically places about 93% of the image on SCA1 and 7% on SCA3. MTI has several commandable options for clock rate and integration time, each having a different responsivity and calibration. The 1370 nm cirrus detection band has duplicate detector arrays to improve the signal-to-noise. An overview of this 37 cm unobscured push-broom instrument and calibration is provided by Clodius et al.[26] A power failure 5 months into the mission caused the loss of all on-board calibration capability and left the aperture door

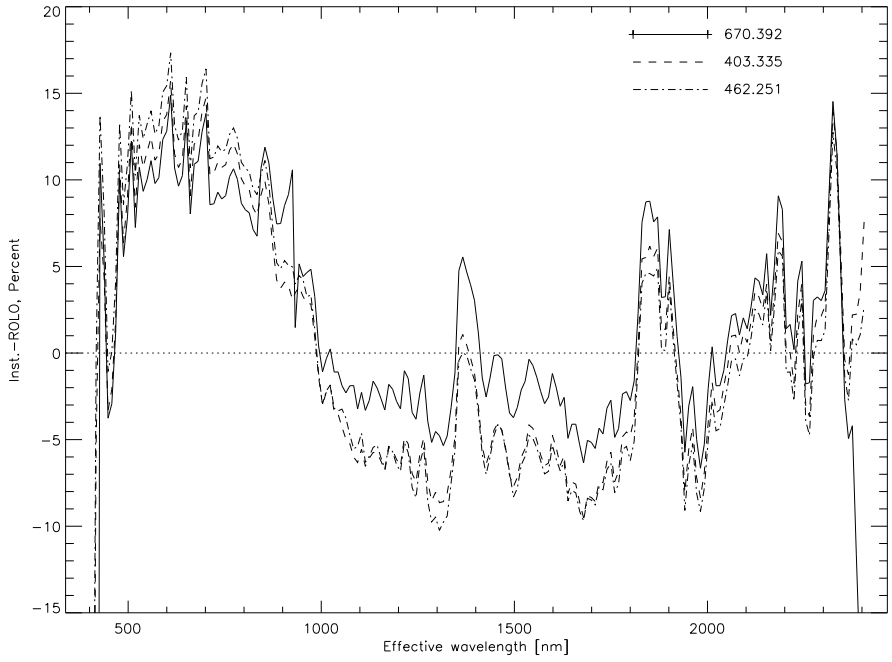

Figure 3. Absolute response of Hyperion for three lunar observations. The response peaks near 1400 nm and 1850 nm have the shape and position of H_2O vapor bands and probably result from absorption in the laboratory calibration path.

Table 4: MTI Band Wavelengths and Irradiance Comparison: post solar exposure.

MTI	Nominal	Effective	Disagreement		<|resid|>
Band	Wavelength	Wavelength	Initial	Drift	
	(nm)	(nm)	%	%/year	
	(nm)	(nm)	0.33	3.73	<– Uncert.
A	480.	489.85	-1.08	-3.17	0.25
B	560.	562.53	-7.98	-5.37	0.25
C	650.	651.50	-3.69	-4.00	0.21
D	810.	802.58	-6.13	-1.83	0.21
E	880.	874.68	-6.24	-1.00	0.14
F	940.	940.98	0.71	-1.25	0.18
G	1010.	1017.32	11.32	3.32	0.16
H	1370.	1382.52	1.04	0.30	0.15
H2	1370.	1382.52	2.61	0.37	0.26
I	1650.	1637.82	-10.39	0.80	0.11
O	2210.	2205.33	-3.29	-6.82	0.20

permanently open. Approximately one year later, 2001 Oct. 31, MTI was inadvertently scanned passed the Sun, causing permanent change to some bands. Lunar views have been used throughout the mission to provide a model-corrected stable radiometric reference useful for tracking system changes; these views have been coupled with terrestrial vicarious calibration campaigns. Comparisons of MTI radiometry with lunar modeling have been instrumental in understanding the performance of the ground calibration data and algorithms along with on-orbit changes in instrument health.

The results for MTI are shown in Table 4 and Fig. 4. Exposure to the sun occurred after the first two runs shown, and marked differences are apparent in the SWIR bands. The drift rate reported in Table 4 is calculated

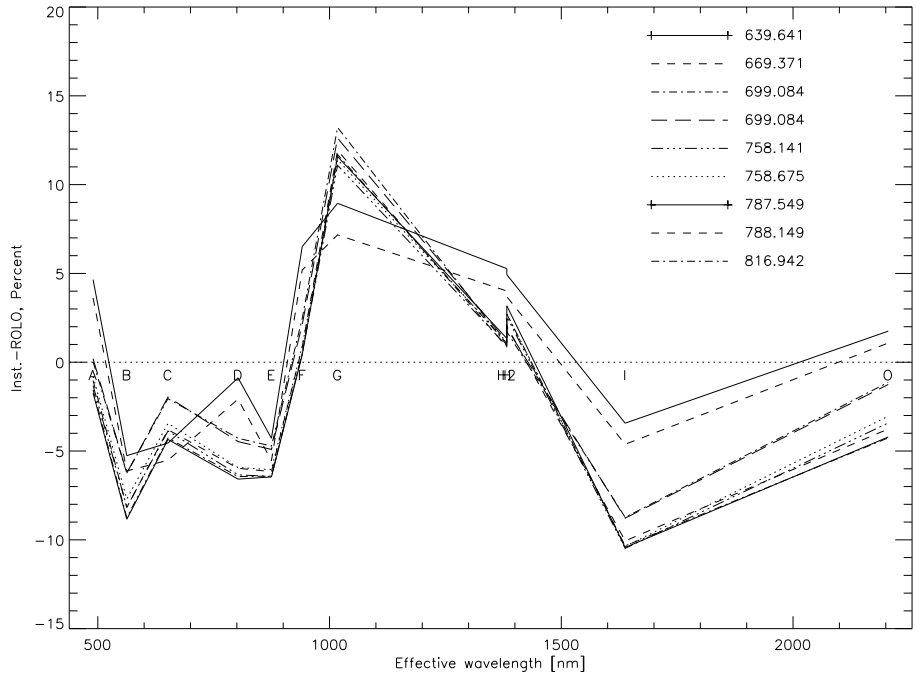

Figure 4. Percent disagreement spectra for MTI; data are shown 9 observations over 7 lunations. The response for the 650 and 1010 nm bands increased between the end of October (day 669) and the end of November 1999. The small offsets at 1400 nm result from independent calibration of the two line arrays in Band H.

subsequent to the exposure and may not be indicative of normal degradation of unexposed surfaces. Telemetry at the time of the exposure suggested the image of the Sun swept past the longwave portion of SCA3 and the VNIR/SWIR portions of SCA2, thus changes in these SCAs may be more severe than indicated by lunar images, which fall mainly on SCA1. The response for the 650 and 1010 nm bands increased between the end of October (Day 699) and the end of November 2001, this is attributed to leakage caused by the solar exposure.

6. SPECTRAL COMPARISON BETWEEN FOUR INSTRUMENTS

The ROLO irradiance model accounts for the variation of the Moon's brightness with geometry and wavelength, and thus enables using the Moon as a known "source" to transfer calibration scales between spacecraft. Observations made by two instruments in similar bands at the same or different times can be compared in terms of the percent disagreement P of Eqn. 4.

The spectrum of P for each instrument derived as the average of all of its observations (except that only MTI observations after solar exposure are used) is shown in Fig. 5. SeaWiFS is within 4% in all bands, generally rising with wavelength over the first 7 bands; ALI is about 3% high below 1300 nm, and MTI has a wide variation of response, being generally low shortward of 900 nm. Hyperion is about 10% high in the VNIR, 5% low in the SWIR, with rapid (spectrally) variations of several percent. All three instruments with response at 1630 nm are roughly 7% lower than the ROLO model.

Some of the differences between instrument radiometric scales may be due to the use of different solar spectral irradiance models by the teams; e.g., ALI and Hyperion both use solar diffusers as part of their calibration activity. Certainly there are differences between the solar irradiance models in common use, such as Wehrli,[11] and Neckel and Labs.[27] These differences exceed the errors in the lunar model and may be limiting comparison accuracy.

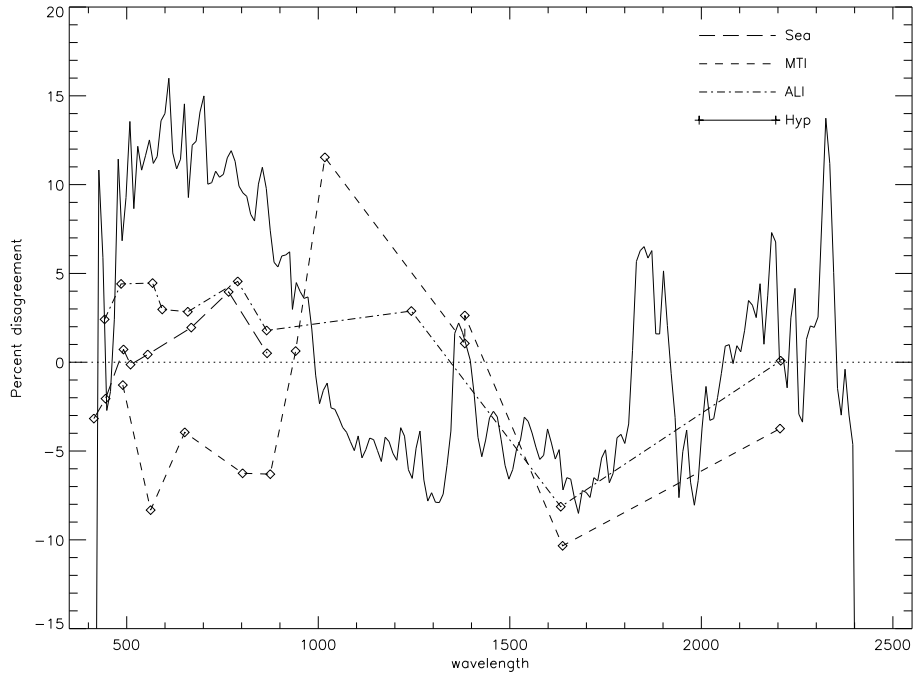

Figure 5. Spectral shape of lunar calibration results for four spacecraft instruments. The curve for each instrument is the average of their individual observations. The differences between instruments are largely independent of the lunar model absolute calibration.

7. CONCLUSIONS

The basic procedures for lunar calibration have been established, and observations of the Moon by orbiting instruments provide the ability to track their response changes with high precision. These observations also give a useful indication of the relative spectral response between bands, which will become an indication of absolute response as the absolute scale of the lunar irradiance model improves. Lunar observations at any time, in conjunction with the lunar irradiance model, allows comparison of response for similar bands between different instruments to the percent level.

Spacecraft teams are gaining experience in processing lunar images to irradiance that can be readily and reliably exchanged, and the method has the potential of reaching the 0.1% level if instruments are that stable. Lunar calibration views have also been found helpful in assessing changes due to "catastrophic" events by eliminating the variability of the atmosphere when attempting to understand some pathologic change to an instrument.

ACKNOWLEDGMENTS

Much of the programming for reduction of the ROLO observations was done by James Anderson and Kris Becker. Bill Atkins has been integral to the calibration of MTI. The ROLO project is supported by Goddard Space Flight Center as part of the NASA Mission to Planet Earth under NASA contract S-41359-F.

REFERENCES

1. H. H. Kieffer and R. L. Wildey, "Absolute calibration of Landsat instruments using the Moon," *Photogramm. Eng. Remote Sens.* **51**, pp. 1391–1393, 1985.
2. H. H. Kieffer and R. L. Wildey, "Establishing the Moon as a spectral radiance standard," *J. of Atmospheric and Oceanic Technology* **13**(2), pp. 360–375, 1996.

3. R. A. Barnes, J. R. E. Eplee, and F. S. Patt, "SeaWiFS measurements of the Moon," *Proc. SPIE* **3438**, pp. 311–324, 1998.
4. R. A. Barnes, J. R. E. Eplee, F. S. Patt, and C. R. McClain, "Changes in the radiometric response of SeaWiFS determined from lunar and solar-based measurements," *Appl. Opt* **38**, pp. 4649–4664, 1999.
5. I. Grant, H. H. Kieffer, and J. M. Anderson, "Lunar calibration of geostationary visible-band images," *Proc. SPIE* **3438**, pp. 337–347, 1998.
6. J. M. Anderson, H. Kieffer, and K. Becker, "Modeling the brightness of the Moon over 350-2500 nm for spacecraft calibrations," *Proc. SPIE* **4169**, pp. 248–259, 2000.
7. H. H. Kieffer, "Photometric stability of the lunar surface," *Icarus* **130**, pp. 323–327, 1997.
8. T. C. Stone and H. H. Kieffer, "Absolute irradiance of the Moon for on-orbit calibration," *Proc. SPIE* **4814**, pp. x–x, 2002.
9. C. Frohlich, "Observations of irradiance variations," *Space Sci. Rev.* **94**, pp. 15–24, 2000.
10. H. H. Kieffer and J. A. Anderson, "Use of the Moon for spacecraft calibration over 350–2500 nm," *Proc. SPIE* **3438**, pp. 325–335, 1998.
11. C. Wehrli, "Spectral solar irradiance data." World Climate Research Program (WCRP) Publication Series No. 7, WMO ITD-No. 149, 1986. pp. 119-126.
12. T. B. McCord and T. V. Johnson, "Lunar spectral reflectivity (.3 to 2.5 microns) and implications for remote mineralogical analysis," *Science* **169**, pp. 854–858, 1970.
13. A. P. Lane and W. M. Irvine, "Monochromatic phase curves and albedos for the lunar disk," *Astronom. J.* **78**, pp. 267–277, 1973.
14. T. B. McCord, R. N. Clark, B. R. Hawke, L. A. McFadden, P. D. Owensby, and C. M. Pieters, "Moon - near-infrared spectral reflectance, a first good look," *J. Geophys. Res.* **86**, pp. 10883–10892, Nov. 10 1981.
15. P. G. Lucey, B. R. Hawke, C. M. Pieters, J. W. Head, and T. B. McCord, "A compositional study of the Aristarchus region of the Moon using near-infrared spectroscopy," *Jour. Geophys. Res.* **91**, pp. D344–D354, 1986.
16. C. M. Pieters, "The Moon as a spectral calibration standard enabled by lunar samples: The clementine example," in *Workshop on New Views of the Moon II: Understanding the Moon Through the Integration of Diverse Datasets. Flagstaff, AZ. Lunar and Planetary Instit. Contrib.*, pp. 47–48, Sept. 1999.
17. H. H. Kieffer, P. Jarecke, and J. Pearlman, "Initial lunar calibration observations by the EO-1 hyperion imaging spectrometer," *Proc. SPIE* **4480**, pp. 247–258, 2002.
18. S. B. Hooker, W. E. Esaias, G. C. Feldman, W. W. Gregg, and C. R. McClain, "An overview of SeaWiFS and ocean color," *NASA Tech. Mem. 104566* **1**, pp. 1–24, 1992.
19. R. A. Barnes and A. W. Holmes, "Overview of the SeaWiFS ocean sensor," *Proc. SPIE* **1939**, pp. 224–232, 1993.
20. R. A. Barnes, W. L. Barnes, W. E. Esaias, and C. R. McClain, "Prelaunch acceptance report for the SeaWiFS radiometer," *NASA Tech. Mem. 104566* **22**, p. 32 pp., 1994.
21. R. A. Barnes and C. R. McClain, "The calibration of SeaWiFS after two years on-orbit," *Proc. SPIE* **3870**, pp. 214–227, 1999.
22. H. H. Kieffer, J. M. Anderson, and K. J. Becker, "Radiometric calibration of spacecraft using small lunar images," *Proc. SPIE* **3870**, pp. 193–205, 1999.
23. R. A. Barnes, R. E. Eplee, G. M. Schmidt, F. S. Patt, and C. R. McClain, "The calibration of SeaWiFS. part 1: Direct techniques," *Applied Optics* **40**, pp. 6682–6700, 2001.
24. J. A. Mendenhall, C. F. Bruce, C. J. Digenis, D. R. Hearn, and D. E. Lencioni, "EO-1 advanced land imager technology validation report." MIT Lincoln Lab. Project Report EO-1-9, June 4 2002.
25. D. Jupp, "Calibration of Hyperion using Lake Frome," 2001. Personal comm.
26. W.B.Clodius, S. Bender, R. R. Kay, B. W. Smith, W. H. Atkins, R. W. Christensen, C. K. Little, E. F. Zalewski, and W. M. Rappoport, "MTI on-orbit calibration," *Proc. SPIE* **3753**, pp. 380–391, 1999.
27. H. Neckel and D. Labs, "The solar radiation between 3300 and 12500 Angstrom," *Solar Physics* **90**, pp. 205–258, Feb. 1984.